JOURNAL GEOLOGICAL SOCIETY OF INDIA
Vol.93, April 2019, pp.399-408

Petrogenesis and Geochemical Evolution of Dhauladhar and Dalhousie Granites, NW Himalayas

Rimpi Dhiman and Sandeep Singh*
Department of Earth Sciences, Indian Institute of Technology Roorkee, Roorkee – 247 667, India
*E-mail: san662005@gmail.com

ABSTRACT

Whole rock geochemical analysis has been carried out on samples from Dhauladhar and Dalhousie granites of the north-western region of Himalayas. The mineral assemblage of these granites is K-feldspar, plagioclase, and biotite, with Dhauladhar granite being richer in plagioclase and biotite than the Dalhousie granites. The Dhauladhar granites are mostly coarse to medium-grained porphyritic, variably mylonatized and biotite bearing whereas, the Dalhousie granites are fine-grained two-mica granites. The silica-rich (SiO_2=64-72 wt %) Dhauladhar granites have a potassic (K_2O/Na_2O> 0.9-1.8) and peraluminous (A/CNK=1.03-1.3) character. Dalhousie granites show a similar character, albeit to a different degree (SiO_2=69-74 wt %), (K_2O/Na_2O > 1.1-1.5) , (A/CNK=1.3-1.7). The Dalhousie granites are richer in, U, Th, and LREE, yet extremely depleted in Sr, Ba, Nb. They have flatter REE patterns with comparatively strong Eu anomaly (Eu/Eu*= 0.02-0.04). The Rb/Ba vs Rb/Sr and CaO/Na_2O vs Al_2O_3/TiO_2 ratios indicate sedimentary source with the psammitic nature for Dhauladhar and pelitic nature for Dalhousie granites. However, the Eu/Eu* value indicates that plagioclase abundance is greater in Dhauladhar granites than in Dalhousie granites. The present study suggests that Dalhousie granites being more evolved than Dahuladhar granites.

INTRODUCTION

The Paleozoic era is marked by voluminous addition of granitic bodies into the continental crust and, the genesis and evolution of these granitic bodies hold valuable information on the origin and evolution of continental crust through the geological times (Kemp and Hawkesworth, 2003; Frost and Frost, 2013). Granitic bodies of Paleozoic age that are exposed in the Himalayas are referred to as Lesser Himalayan Granitic belt (LHGB) (LeFort et al. 1983; Frank et al., 1977; DeCelles et al., 2000; Miller et al., 2001; Singh and Jain, 2003; Cawood et al., 2007). This Lesser Himalayan Granitic Belt (LHGB) is exposed within the Lesser Himalayas (geographically) but are the part of Higher Himalayan Crystallines (HHC) and occurs all along the Himalayas from the Besham in Swat valley (NW Himalayas) to the Bomdila gneiss in Arunachal Pradesh (NE Himalayas) (Singh, 2005; Singh and Jain, 2003). These granites are pre-Himalayan granitic suites showing broad similarity in geochemistry and petrological characteristics to each other. Both S-type granites with similar syn-collision tectonic setting (Le Fort et al., 1987; Singh and Jain, 2003). However, detailed geochemical and isotopic data indicate that these bodies often mark a complicated history of multistage and hybrid processes (Sylvester, 1998; Patiño Douce, 1997, 1999; Singh and Jain, 2003; Cawood et al., 2007).

In this study, the magma sources and the petrogenitic process of Dhauladhar and Dalhousie granites are discussed and the relationship between their generation and evolution by whole-rock geochemical analysis (major and trace elements) is ascertained.

GEOLOGY OF THE REGION

The Dalhousie and the Dhauladhar granites are named after their respective geographic locations in the study area (Le Fort, 1986). The Dhauladhar and the Dalhousie granites are part of the Lesser Himalayan granitic belt (LHGB). The Dhauladhar granites are situated in the southern slopes of the Dhauladhar range. Petrographically these granites are medium to coarse-grained and exhibit gneissose to porphyritic texture. The intense ductile deformation associated with Himalayan orogeny has resulted in mylonitization of these granites (Le Fort, 1983; Singh and Jain, 1996; Singh et al., 2002; Singh, 2003; Singh and Jain, 2003).

Geologically the Dhauladhar region is characterized by multiple events of metamorphism and deformations, both pre and post-Himalayan. From south to north, the Precambrian to Cenozoic metasedimentary, sedimentary, and volcanic rocks of the area are divided by three major tectonic boundaries: the Drini thrust, the MBT (Main Boundary Thrust) and the MCT (Main Central Thrust), locally known as Panjal thrust (Fig 1). The southernmost of these, the Drini thrust, separates the Tertiary sedimentary Shiwalik rocks in the south from the Dharamshala Formation in the north. The Dharamshala Formation is characterized by micaceous sandstones inter-bedded with clay sediments of four varieties (viz., crimson red, green, maroon and red color combinations) (Nautiyal et al., 1952). The MBT thrusts the Dharamshala traps over the north of Dharamshala Formation. Dharamshala traps are in turn thrust over by the Precambrian metasedimentary rocks of the Salkhala Formation across the Panjal thrust. The Dhauladhar and Dalhousie granites of Paleozoic age occur within the Salkhala Formation.

The Dalhousie granite exposed in Dalhousie town which is situated in the NW of Dhauladhar granites is a light coloured, massive, and homogeneous granitic body and is petrographically, a medium-grained rock with biotite, muscovite and abundant large phenocrysts of K-feldspar. Muscovites are present in the center of the pluton and the biotites are concentrated along the margins (Mukherjee et al. 1998; Lahoti et al. 2017). The granitic body shows a sharp intrusive contact with the country rock. On the basis of the contrasting physical appearance, the Dalhousie granites have been divided into two units' viz., (i) western granitic bodies and (ii) main granitic body (Eastern granites) (Bhatia and Kanwar, 1973). The western granitic bodies are also referred as "outer granite bands" occur in the carbonaceous shale belt of the Panjal traps; are also thrust over by the schist, phyllite, and quartzite of the Salkhala Group (McMohan, 1881; Thakur et al. 1995). The main granitic body is divided into eastern granite (Kumar and Bhatia, 1975) and "inner granitic band" (McMohan, 1881). The study area falls within the inner granitic band. The granites from this unit have "a typical granitic composition and are comprised of quartz, feldspar (orthoclase and microcline). At places, the granitic bodies occur as aplites representing as the last phase of the magma to crystallize.

Field observation in Dhauladhar granites shows mylonitic texture

0016-7622/2019-93-4-399/$ 1.00 © GEOL. SOC. INDIA | DOI: 10.1007/s12594-019-1194-9

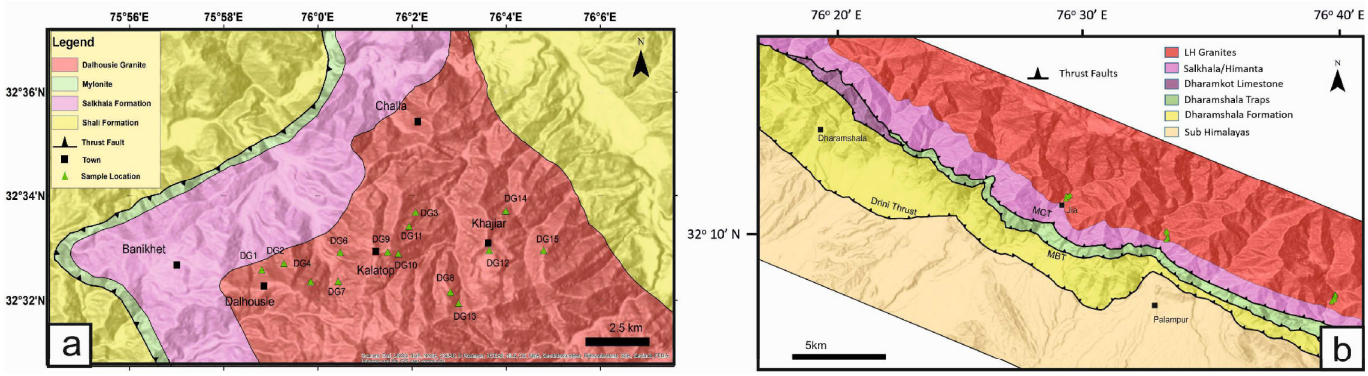

Fig.1. Geological map of the study area **(a)** geological map of Dalhousie area modified (after Bhatia and Kanwar. 1990 and Mukherjee et al., 1998) with sample locations for geochemical analysis dates. **(b)** Geological map of the Dharamshala–Baijnath area (after Mahajan. 1991).With sample locations for geochemical analysis.

(Fig 2a) as a result of intense ductile deformation during Himalayan orogeny. The exposure of these bodies suggest the extremely deformed charasterstic not only at the margins but continues along the exposure. However, Dhalhousie granites show typical granitic texture (Fig 2b,c). Apart from textural difference, the darker minerals content are less in Dalhousie granites as compared to Dhauladhar granites.

Detailed petrographic studies show that both Dhauladhar and Dalhousie granites are composed of K-feldspar, plagioclase, quartz, muscovite, biotite and tourmaline along with accessory minerals like zircon and apatite. Plagioclase and K-feldspar crystals are > 2 mm in size. However, the modal percentage of plagioclase is comparatively higher than K-feldspar in Dhauladhar granites and the reverse is true for Dalhausie granites. Samples from both the locations show perthetic texture along with the inclusions of quartz and plagioclase (Fig 3i). In most of the samples quartz shows undulose extinction with sutured crystal boundaries (Fig 3b), indicating that the rocks experienced stress during or after emplacement (Fig. 3d,f). Tourmaline present in Dhauladhar granites shows sharp zoning (Fig.3c,g). Biotite is dominant ferromagnesium mineral in Dhauladhar granite having dark brown to medium brown colour. The ferromanganese mineral-rich parts of the Dhauladhar granite form melanocratic bands which alternate with the silica-rich leucocratic bands. In contrast, the ferromagnesium minerals do not form separate bands in the Dalhousie granite and appear to be disseminated within the rock. At some places, especially in Dhauladhar granite, biotite has been altered to chlorite (Fig.3d).

ANALYTICAL TECHNIQUE

Whole rock geochemical analysis has been made on twenty-six (26) fresh granitic samples from both Dhauladar and Dalhousie granites. The samples have been crushed and powdered using jaw crusher and Retsch Disc Mill in sample preparation laboratory at the Department of Earth Sciences, IIT Roorkee. Major elements were analyzed at Wadia Institute of Himalayan Geology and trace elements were analyzed at Institute Instrumentation Center at Indian Institute of Technology, Roorkee. For Major elements, pressurized pellets were prepared and X-ray fluorescence spectrometry (XRF), a study was performed at 12kv tube voltage and, 40 µA tube current in VAC with no filtered path. The samples were subjected to a lifetime of 200 seconds. The emission intensity of the radiation was measured with the suitable X-ray spectrometer using international reference standards JG-1a. The detailed protocol has been described by Satyanarayanan et al. (2014). The accuracy and precision of the XRF data with standard (JG-1a) are better than ±0.5%. The trace element and REEs concentrations were determined using an ELAN DRC-e (Perkin Elmer) Inductively Coupled Plasma Mass Spectrometer (ICP-MS). The digestion process has been followed as per the lab established protocol in TIMS (Thermal Ionization Mass Spectrometry) lab at the Institute Instrumentation Center at Indian Institute of Technology Roorkee. The analytical error in results for the standard (GSP-2, BCR-2 USGS, USA) is better than 5%.

RESULTS

Whole-rock major- and trace-element analytical data are given in (Table 1). The average silica content ranges from (64-72 wt %) for Dhauladhar granites and (69-74 wt %) for Dalhousie granites. The differentiation index (D.I.) increases systematically from least differentiated Dhauladhar granites to Dalhousie granites (Fig 4a). The AFM diagram shows the calc-alkaline enrichment trend (Fig 4). The Harker diagrams (Fig. 5) shows generally smooth, coherent trends of oxide enrichment and depletion from Dhauladhar to Dalhousie. The plots show a systematic increase in Al_2O_3, K_2O, and P_2O_5 and decrease in CaO, Fe_2O_3, MgO, TiO_2, MnO with increasing SiO_2. The extremely positive trend of K_2O (Fig. 5) along with the moderate positive correlation of Na_2O+ K_2O with SiO_2 indicates the evolution in the

Fig.2. Field photographs of Dalhousie and Dhauladhar granites **(a)** Dhauladhar mylonetised with big porphyroblasts of feldspars (location 32°7'29.9": 76°39'35.4").**(b)** Quartz vein in Dalhousie granites. **(c)** Dalhousie granites with fine-grained vein.

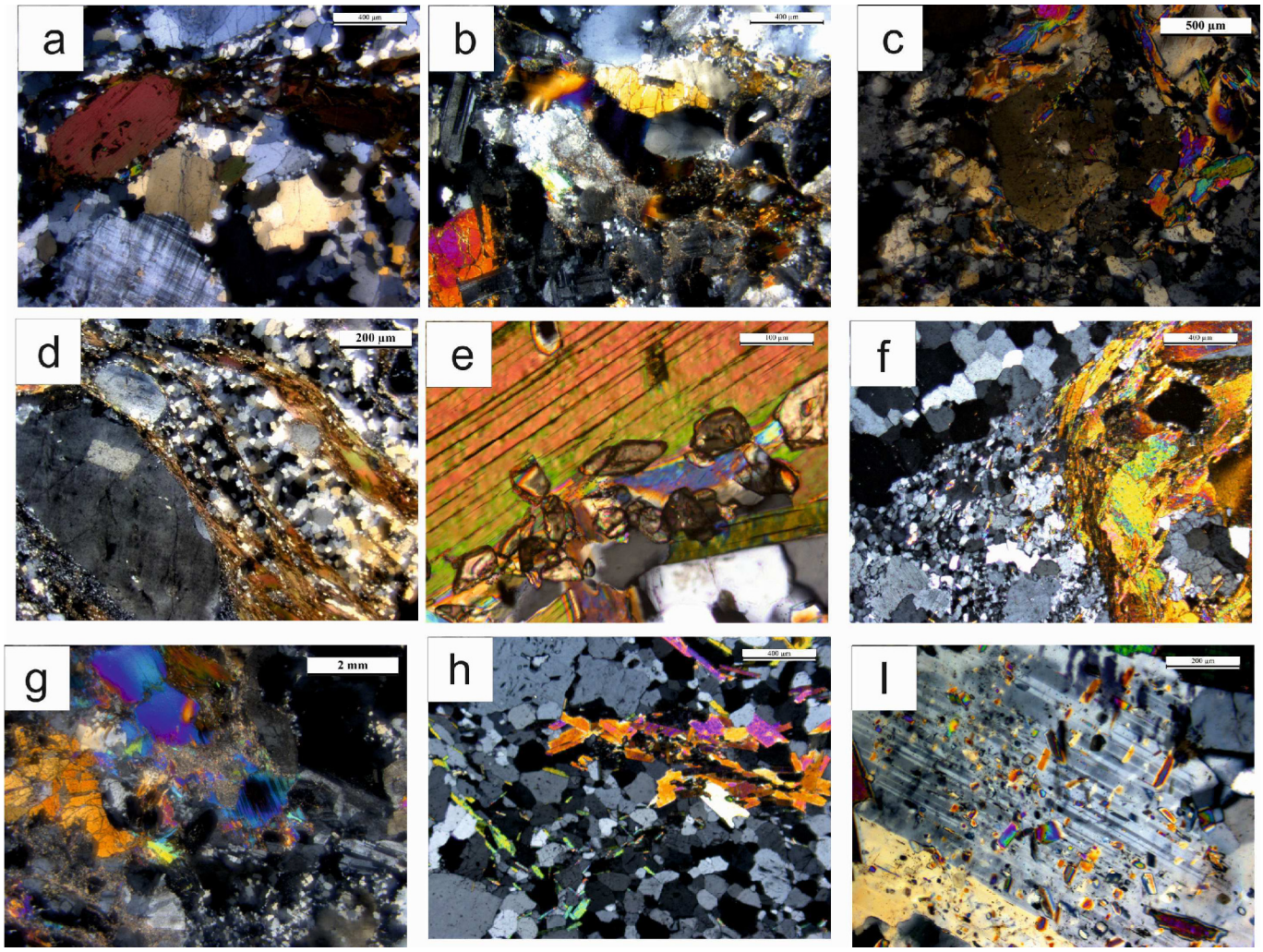

Fig.3. Photomicrographs of Dhauladhar and Dalhousie granites showing **(a)** alignment of microcline phenocryst, biotite, muscovite along with the anhydral quartz grains. **(b)** recrystallized quartz grains. **(c)** Altered plagioclase phenocryst in the matrix of fine-grained quartz and mica. **(d)** Elongated and deformed twin feldspar porphyroclast along with quartz, muscovite, biotite and chlorite in the matrix shows the two different events of deformations. **(e)** Alignment of zircon grains in biotite. **(f)** extremely fine grains, feldspar, and muscovite forming localized micro-shear zone. **(g)** Tourmaline crystal with quartz. **(h)** Sample from Dalhousie granite shows fine to medium grain. (i) Feldspar grain shows the perthite texture with the inclusions. All the photographs are taken under cross Nicoles, PPL abbreviations (Qtz) quartz, (Pl) plagioclase, (Mus) muscovite, (Bt) biotite, (Tur) tourmaline, (Zr) Zircon.

subalkaline field. All samples are peraluminous in composition with A/CNK (molar Al_2O_3/CaO+ Na_2O+ K_2O) A/CNK (Avg. 1.09) (Table1).

On primitive mantle normalized multi-element spider diagram (Fig 7), all the samples show similar trace element distribution patterns. Enrichment of LILE (Cs.Rb, Th, U) to HFSE (Nb, Ti), high Rb, Th as compared to Nb and large negative Ba anomaly represent the crustal dominance patterns (Fig.7) (Thirwall & Jones,1983). However, as compared to Dhauladhar granites, Dalhousie granites display higher Rb and Rb/Sr (4.99-66.9) ratios and lower Sr content. The trace elements variation trends, of both Dhauladhar and Dalhousie granites, are scattered and show less correlation with SiO_2. The scattering in the variation diagram of both major and trace elements shows the fractionation as well as the heterogeneity in the source (Rollinson, 2014). As shown in (Fig. 6) Sr, Ba, Zr, show a nearly decreasing trend as we go from Dhauladhar to Dalhousie. However, Rb shows nearly increasing trend from Dhauladhar to Dalhousie, while other show scattered or minor change in their trends. Chondrite-normalized REE diagrams (Fig.8) show moderate to less negative Eu anomalies (0.04-0.05) moderately flat LREE patterns (La_N/Sm_N =1.9-2.8) and nearly flat to positive HREE patterns (Gd_N/Yb_N=0.69-2.4). Dhauladhar granites display a relatively narrow range, with (ΣREE 31-124). In contrast, the REE patterns of Dalhousie granite show a more variation (ΣREE 34-174) and relatively stronger negative Eu anomaly (Eu/Eu*= 0.01-0.03).

DISCUSSION

The composition of a source rock, its partial melting conditions and the magma evolution processes (magma mixing and fractional crystallization and assimilation) are the major factors, which affect the geochemical characteristics of the granites (Clemens and Stevens., 2012; Collins and Sawer., 1996; De Paolo, 1981; Gao et. al, 2014). All the geochemical features of Dhauladhar and Dalhousie granites contain Al-rich minerals (muscovite and biotite) with high SiO_2 indicate S-type characteristics of the granites, derived from a melt of metasedimentary source in upper crust (Chappell and White, 1992, 2001; Clemens, 2003; Healy et al., 2004). The samples from the Dhauladhar granites show peraluminous to weakly peraluminous (A/CNK) character (Table 1) with the high CaO/Na_2O (>0.3) ratios and comparatively high Sr content (Fig.10), indicating more mature plagioclase-rich psammatic source (Chappell and White, 2001). On the other hand, high Al_2O_3/TiO_2 and low CaO/Na_2O (< 0.3) ratio

Table 1. Major and trace elemental data of Dalhousie and Dhauladhar granites

	Dalahausie granites													Dhauladhar granites											
Sample	DG2/ 2	DG3/ 3	DG4/ 4	DG6/ 6	DG7/ 7	DG9/ 9	DG10/ 10	DG11/ 11	DG12/ 12	DG13/ 13	DG14/ 14	DG15/ 15	DG18/ 18	DP1/ 1	DP3/ 3	DP4/ 4	DP6/ 6	DP7/ 7	DP8/ 8	DP10/ 10	DP11/ 11	DP12/ 12	DP13/ 13	DP14/ 14	DP15/ 15	DP16/ 16
Major Element																									
SiO_2	69.08	71.10	71.50	71.00	71.11	73.74	73.60	74.42	68.21	73.00	69.17	73.03	74.42	70.42	71.60	68.03	67.34	69.33	68.89	69.75	69.48	72.11	71.03	67.82	64.56	66.80
TiO_2	0.10	0.27	0.21	0.16	0.16	0.17	0.13	0.21	0.15	0.15	0.13	0.14	0.07	0.60	0.63	0.59	0.30	0.53	0.41	0.60	0.56	0.39	0.32	0.40	0.28	0.28
Al_2O_3	17.14	16.20	15.57	16.43	16.24	15.21	15.28	15.41	18.03	15.65	16.43	15.37	14.95	15.22	16.57	15.86	15.14	13.59	16.02	15.11	14.70	15.64	15.75	14.52	14.90	14.81
Fe_2O_3	1.05	2.31	1.78	1.64	1.59	1.77	1.46	2.02	1.89	1.56	1.44	1.41	0.91	4.49	4.75	4.46	2.51	4.23	3.12	4.50	4.49	3.31	2.83	3.16	2.63	2.58
MgO	0.12	0.26	0.49	0.18	0.17	0.19	0.18	0.25	0.56	0.26	0.19	0.23	0.10	0.89	1.04	0.96	0.08	0.49	0.28	0.88	0.78	0.41	0.35	0.28	0.23	0.26
MnO	0.04	0.04	0.03	0.04	0.03	0.04	0.04	0.04	0.02	0.03	0.03	0.03	0.03	0.05	0.05	0.05	0.03	0.05	0.04	0.05	0.06	0.04	0.04	0.04	0.04	0.04
CaO	0.45	0.78	0.50	0.68	0.64	0.47	0.50	0.40	0.37	0.40	0.54	0.43	0.32	3.07	2.98	2.49	1.57	1.85	2.18	3.09	2.16	2.07	1.08	1.89	1.05	1.07
Na_2O	4.02	3.66	3.44	3.83	3.86	3.45	3.81	2.85	2.90	3.69	3.67	3.43	3.62	3.42	3.27	2.64	2.97	2.60	3.62	3.37	2.87	3.23	2.76	2.95	2.85	2.84
K_2O	4.48	4.31	3.47	5.06	5.08	4.42	4.38	3.98	4.58	4.60	5.19	5.15	4.99	3.28	3.75	4.51	5.42	3.99	4.83	3.26	4.21	4.52	4.88	4.95	4.51	4.52
P_2O_5	0.35	0.24	0.24	0.28	0.26	0.25	0.25	0.22	0.29	0.29	0.29	0.26	0.25	0.32	0.19	0.19	0.15	0.20	0.17	0.32	0.20	0.18	0.19	0.16	0.18	0.18
SUM	96.83	99.17	97.23	99.30	99.14	99.71	99.63	99.80	97.00	99.63	97.08	99.48	99.66	99.16	97.79	98.55	98.60	99.13	98.70	98.52	99.36	98.68	97.95	97.83	98.78	97.61
LOI	1.25	1.24	1.39	1.26	1.05	1.00	1.25	1.06	1.77	1.68	1.18	0.98	1.07	1.07	1.38	1.56	1.02	1.37	1.29	1.50	1.59	1.26	1.19	1.34	1.07	1.11
Q	28.56	32.33	37.82	28.70	28.58	36.46	34.32	42.38	33.82	33.90	27.63	33.19	34.27	29.68	25.33	29.37	29.46	37.78	24.27	29.59	32.45	28.88	33.20	29.76	36.49	35.45
Or	26.20	24.87	19.38	29.49	29.63	25.68	25.47	22.94	25.78	26.59	30.23	29.90	29.26	17.33	19.79	24.45	31.83	22.47	27.93	17.21	23.10	25.78	28.05	28.64	26.13	26.09
Ab	34.01	30.97	29.11	32.41	32.66	29.19	32.24	24.12	24.54	31.22	31.05	29.02	30.63	28.97	27.69	22.37	25.16	22.03	30.64	28.48	24.29	27.31	23.39	24.96	24.14	24.00
An	0.00	2.30	0.91	1.54	1.48	0.70	0.85	0.55	0.00	0.09	0.78	0.44	0.00	13.14	13.52	11.12	6.80	7.89	9.73	13.24	9.40	9.10	4.14	8.34	4.07	4.17
Trace Element																										
V	3.74	2.72	12.41	7.75	7.02	7.77	5.96	9.00	6.46	6.54	6.23	6.70	2.53	57.00	62.00	59.00	27.00	37.00	45.00	59.00	54.00	38.00	29.00	36.00	26.00	12.00
Cr	2.81	17.78	1.40	0.94	0.62	1.49	2.86	1.95	1.02	1.43	1.40	0.64	6.19	42.00	49.00	45.00	32.00	37.00	36.00	42.00	39.00	34.00	40.00	18.00	27.00	22.00
Co	27.21	4.27	33.39	20.05	14.83	18.75	24.83	26.91	22.27	20.23	20.10	21.10	16.92	41.00	40.00	39.00	34.00	49.00	51.00	40.00	71.00	56.00	39.00	51.00	78.00	79.00
Cu	3.40	4.27	4.43	3.09	3.40	12.46	3.74	4.88	1.89	1.16	5.92	5.61	1.12	20.00	18.00	13.00	9.00	9.00	9.00	15.00	13.00	12.00	19.00	11.00	11.00	9.00
Rb	496.65	378.02	287.85	324.92	278.95	311.99	281.05	264.95	260.25	240.96	322.82	281.84	500.74	167.00	180.00	196.00	281.00	242.00	276.00	171.00	237.00	230.00	336.00	265.00	318.00	352.00
Cs	61.57	59.94	36.69	41.67	33.64	32.34	34.74	33.57	29.85	23.37	40.62	30.69	42.82	5.00	5.00	4.00	13.00	9.00	13.00	7.00	7.00	5.00	14.00	10.00	10.00	39.00
Ba	35.69	106.37	57.37	229.43	210.48	121.41	128.53	130.67	98.42	169.00	166.60	187.95	19.04	460.00	490.00	678.00	460.00	497.00	242.00	460.00	403.00	437.00	298.00	411.00	279.00	158.00
Th	4.89	26.04	16.03	8.09	6.48	6.47	7.43	8.52	5.63	7.02	5.76	6.76	4.08	17.00	33.00	27.00	14.00	40.00	53.00	25.00	42.00	24.00	33.00	36.00	33.00	11.00
U	2.23	4.84	3.12	2.74	2.11	1.91	2.29	1.95	1.71	1.70	1.78	1.41	3.82	1.00	5.00	1.00		5.00	6.00	2.00	7.00	5.00	3.00	4.00	8.00	1.00
Nb	10.75	13.44	14.66	11.50	14.64	17.48	20.77	15.50	17.38	6.92	5.65	13.49	15.11	18.00	17.00	17.00	14.00	20.00	22.00	18.00	19.00	16.00	21.00	16.00	18.00	16.00
Pb	11.47	20.32	12.17	28.90	28.06	19.96	17.38	17.54	5.47	13.27	23.10	18.62	6.76	39.00	39.00	44.00	37.00	61.00	37.00	33.00	40.00	39.00	37.00	51.00	38.00	41.00
Sr	16.21	32.88	17.36	60.98	55.81	31.39	34.22	32.09	20.05	29.30	41.94	40.49	7.48	171.00	194.00	172.00	110.00	135.00	87.00	170.00	123.00	140.00	94.00	120.00	94.00	57.00
Hf	0.94	0.98	0.92	0.89	0.81	0.79	0.94	0.98	0.91	0.88	0.77	0.87	0.71	1.12	1.49	1.65	0.97	0.82	0.91	1.25	1.11	0.89	1.63	1.65	0.93	0.79
Zr	34.17	39.16	41.66	10.68	22.57	22.70	28.68	22.33	27.31	14.77	11.42	23.84	21.95	268.00	273.00	252.00	187.00	232.00	303.00	272.00	314.00	188.00	158.00	226.00	151.00	72.00
Rare Earth Element																										
La	5.11	29.17	20.15	13.40	9.86	9.76	11.37	12.85	8.14	9.24	9.53	9.81	4.10	11.37	4.90	13.12	5.17	20.07	15.48	7.98	17.15	7.60	8.03	8.34	10.80	3.77
Ce	11.28	66.41	44.80	28.29	21.30	21.27	24.29	26.33	17.29	20.59	20.38	21.16	9.84	22.58	10.26	26.24	10.50	41.00	30.63	16.63	33.93	16.39	17.17	17.75	22.83	8.41
Pr	1.41	8.02	5.29	3.31	2.52	2.60	2.91	3.24	2.07	2.46	2.43	2.55	1.21	2.68	1.14	2.92	1.16	4.49	3.42	2.28	3.71	1.96	1.93	2.01	2.64	1.04
Nd	5.46	31.81	20.26	12.47	9.54	10.09	11.09	12.73	7.79	9.64	9.57	9.98	4.75	10.70	4.80	12.45	4.19	18.21	12.86	7.90	14.41	7.60	7.91	8.49	10.87	3.81
Sm	1.48	6.91	4.63	3.47	2.76	2.73	2.87	3.47	2.18	2.76	2.61	2.71	1.36	2.35	0.91	2.26	0.92	3.38	2.69	2.08	2.82	1.60	1.44	1.49	1.95	0.91
Eu	0.11	0.37	0.28	0.53	0.46	0.33	0.34	0.35	0.37	0.40	0.40	0.39	0.05	0.60	0.18	0.49	0.22	0.40	0.63	0.86	0.54	0.44	0.23	0.24	0.38	0.26
Gd	0.93	4.10	2.71	2.18	1.71	1.83	1.77	2.19	1.46	1.73	1.73	1.71	0.88	2.84	1.00	2.59	1.12	3.97	2.84	2.23	3.23	1.69	1.50	1.50	2.01	0.88
Dy	1.24	4.06	2.91	2.37	1.78	2.31	1.85	2.53	1.54	1.99	1.94	1.93	1.53	1.86	0.51	1.39	0.73	2.19	1.55	1.54	1.87	1.18	0.67	0.66	0.89	0.45
Ho	0.21	0.77	0.56	0.42	0.31	0.42	0.36	0.44	0.27	0.37	0.36	0.34	0.33	0.50	0.10	0.29	0.18	0.44	0.42	0.63	0.43	0.35	0.15	0.13	0.24	0.19
Yb	0.47	1.59	1.33	0.72	0.60	0.90	0.84	0.84	0.56	0.61	0.73	0.61	1.04	1.30	0.27	0.79	0.51	1.37	1.01	1.13	1.18	0.76	0.42	0.38	0.56	0.35
Lu	0.07	0.20	0.17	0.09	0.07	0.11	0.10	0.10	0.06	0.07	0.10	0.08	0.13	0.26	0.03	0.09	0.08	0.15	0.23	0.44	0.21	0.21	0.08	0.06	0.15	0.14
Y	6.81	21.45	15.08	10.68	8.21	11.01	9.35	11.73	7.63	9.40	9.54	9.04	8.88	59.00	38.00	32.00	42.00	29.00	53.00	59.00	41.00	42.00	17.00	25.00	16.00	11.00
LREE/HREE	2.55	4.44	4.19	3.73	3.66	2.82	3.71	3.31	3.28	3.18	3.12	3.40	1.67	0.76	0.56	1.55	0.50	2.36	1.11	0.58	1.51	0.77	1.85	1.38	2.49	1.40
Eu*	4.49	18.93	13.42	15.21	12.72	10.16	10.93	11.99	9.97	11.79	11.15	11.44	3.24	11.16	3.59	9.58	4.11	8.33	12.83	16.25	10.70	8.71	5.03	5.40	7.97	5.36
La/Lu n	8.30	16.02	12.73	15.72	14.87	9.23	11.89	13.79	13.78	13.75	10.53	12.66	3.29	4.72	17.95	15.99	6.63	14.13	7.17	1.96	8.80	3.92	11.25	15.13	7.59	2.83

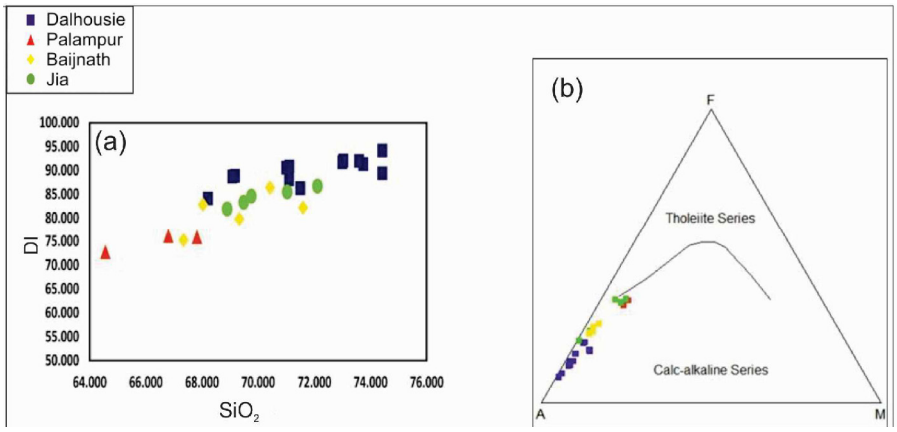

Fig.4. (a) Differentiation index (D.I.) increases vs SiO_2. **(b)** AFM diagram show calc alkaline nature of granites (Irvine and Baragar 1971).

(Fig.10) in the Dalhousie granites indicate a less mature metapelitic source for these granites (Sylvester, 1998; Jung and Pfander, 2007). The inhomogeneity in the source rock is also reflected by the initial $^{87}Sr/^{86}Sr$ ratios, where the initial $^{87}Sr/^{86}Sr$ ratios of Dhauladhar granites is $^{87}Sr/^{86}Sr$ = (0.71947±0.72404) (Chaudhry,1996) and (0.7698±0.0041) for Dalhousie granites (Kansal et al.,2003). Nevertheless, similar primitive mantle-normalized spider diagrams and similar chondrite-normalized REE patterns indicate that these granites were formed in a similar tectonic setting.

The peraluminous granites can be produced by partial melting of crustal rocks under fluid-absent and water present conditions (Patiño Douce and Beard, 1996; Singh and Johannes, 1996; Watkins et al., 2007). The partial melting of metapelites under water present conditions makes plagioclase less stable than mica (Conrad et al., 1988; Watkins et al., 2007; Weinberg and Hasalova, 2015). The fluid flux melting consumes a greater proportion of the plagioclase than muscovite. Therefore, the granitic magma generated under water present conditions have higher An-Ab component compared to Or and higher Eu/Eu*. Micas are rich in Rb and poor in Sr content, whereas the plagioclase is rich in Sr and poor in Rb (Inger and Harris, 1993; Harris and Inger, 1992), implying that the melts derived from the muscovite dehydration melting should exhibit higher Rb/Sr ratios than the melts derived from melting in presence of water. Because Ba has high incompatibility with K-feldspar (Zheng et al., 2005), Ba

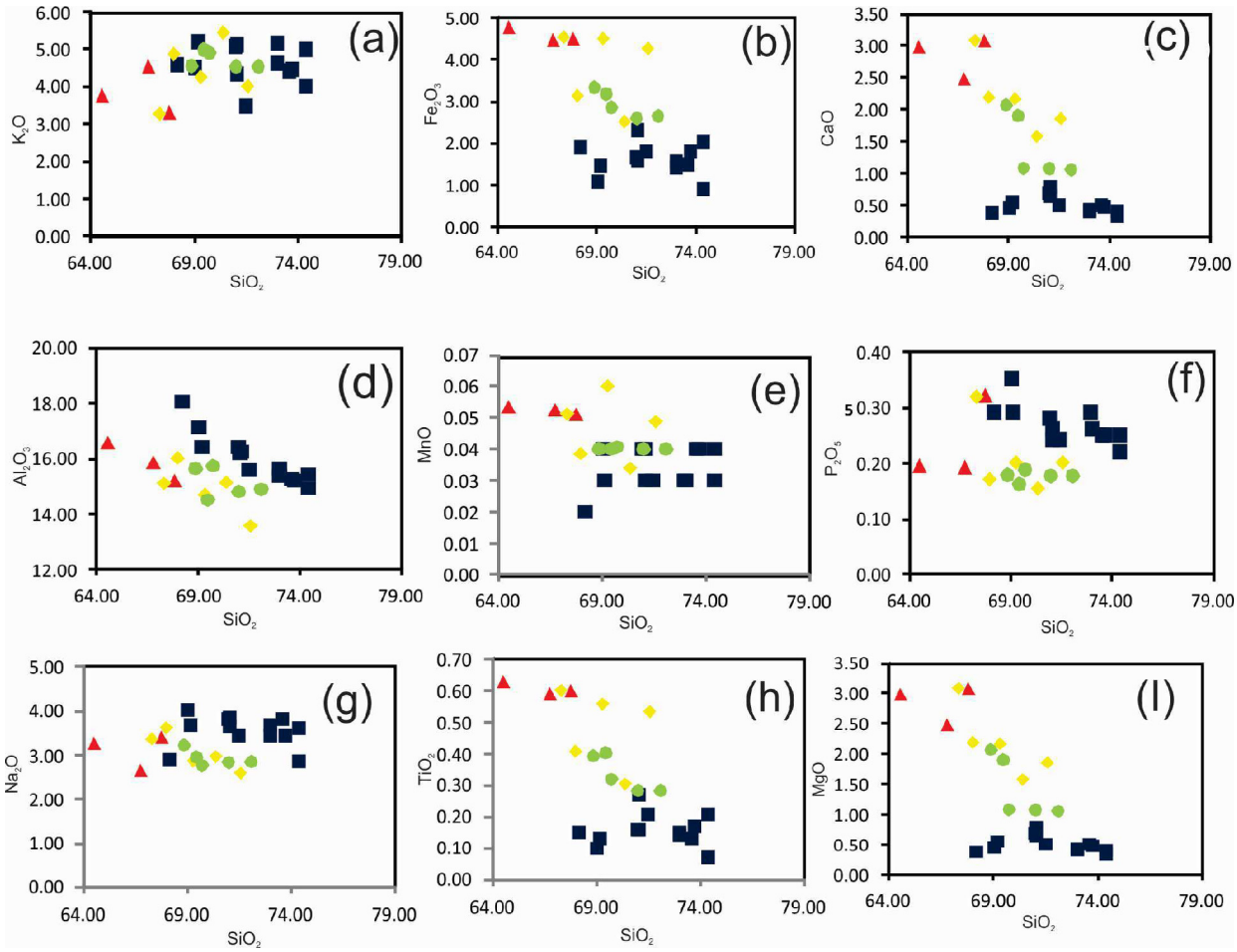

Fig.5. Major elements Harker variation plot of Dalhousie and Dhauladhar granites showing the correlation between SiO_2 and **(a)** K_2O, **(b)** Fe_2O_3, **(c)** CaO, **(d)** Al_2O_3, **(e)** MnO, **(f)** P_2O_5, **(g)** Na_2O, **(h)** TiO_2, **(i)** MgO .

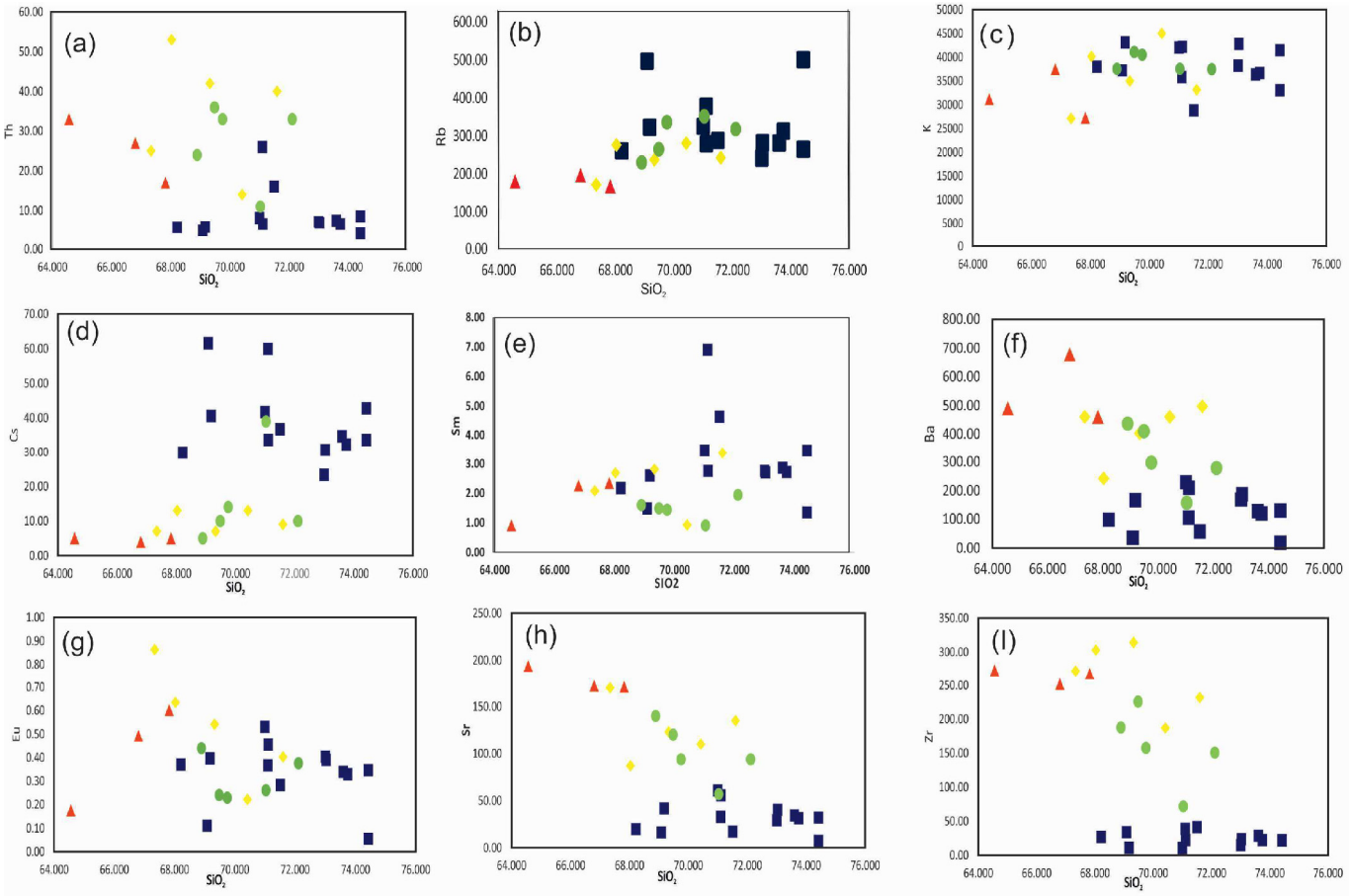

Fig.6. Trace elements Harker variation plot of Dalhousie and Dhauladhar granites showing the correlation between SiO_2 and **(a)** Th, **(b)** Rb, **(c)** K, **(d)** Cs, **(e)** Sm, **(f)** Ba, **(g)** Eu, **(h)** Sr, **(i)** Zr.

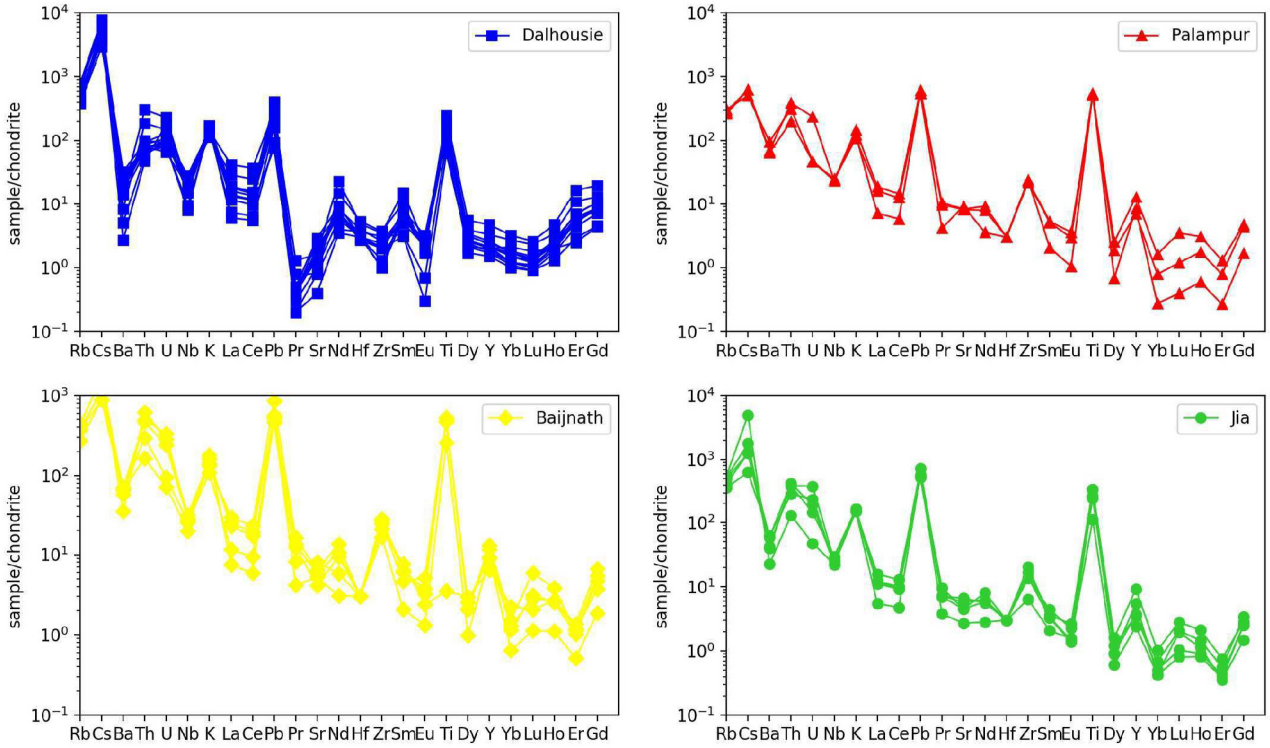

Fig.7. Primitive mantle-normalized trace element spider diagrams primitive mantle normalized values are from Sun and McDonough (1989).

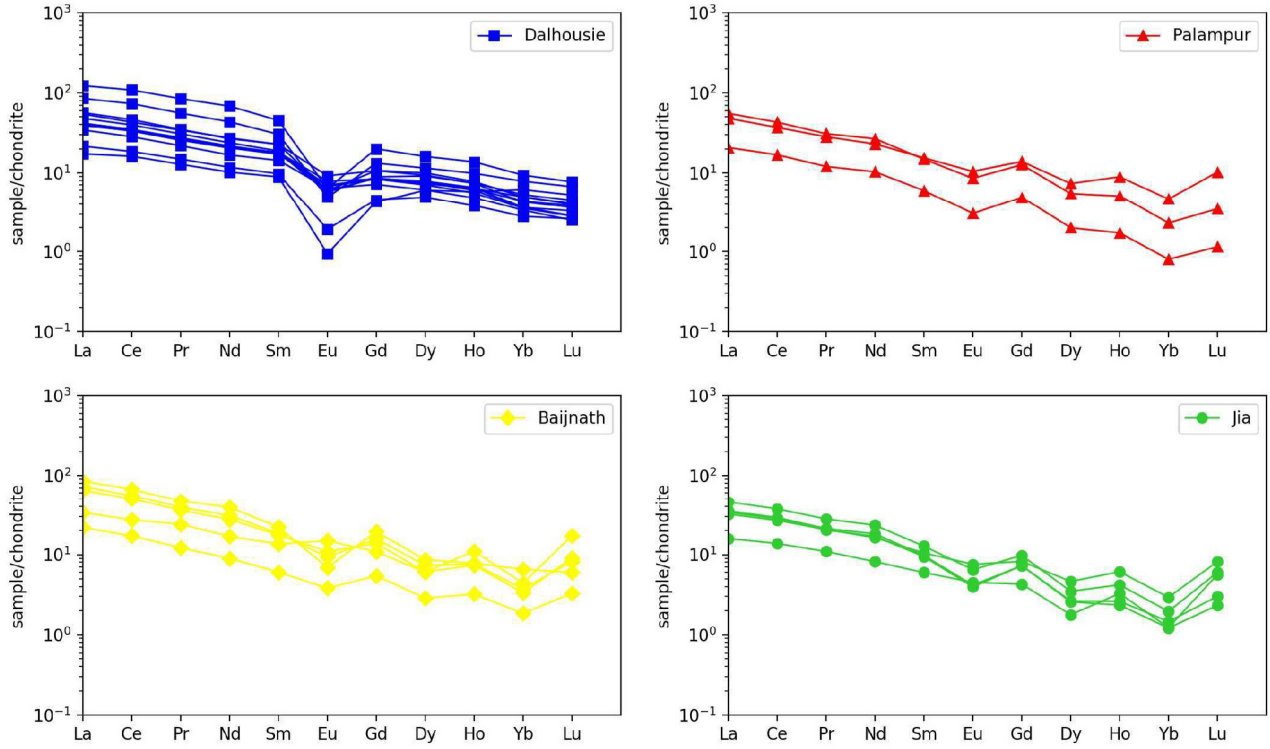

Fig.8. Chondrite-normalized trace element spider diagrams primitive mantle normalized values are from Sun and McDonough (1989).

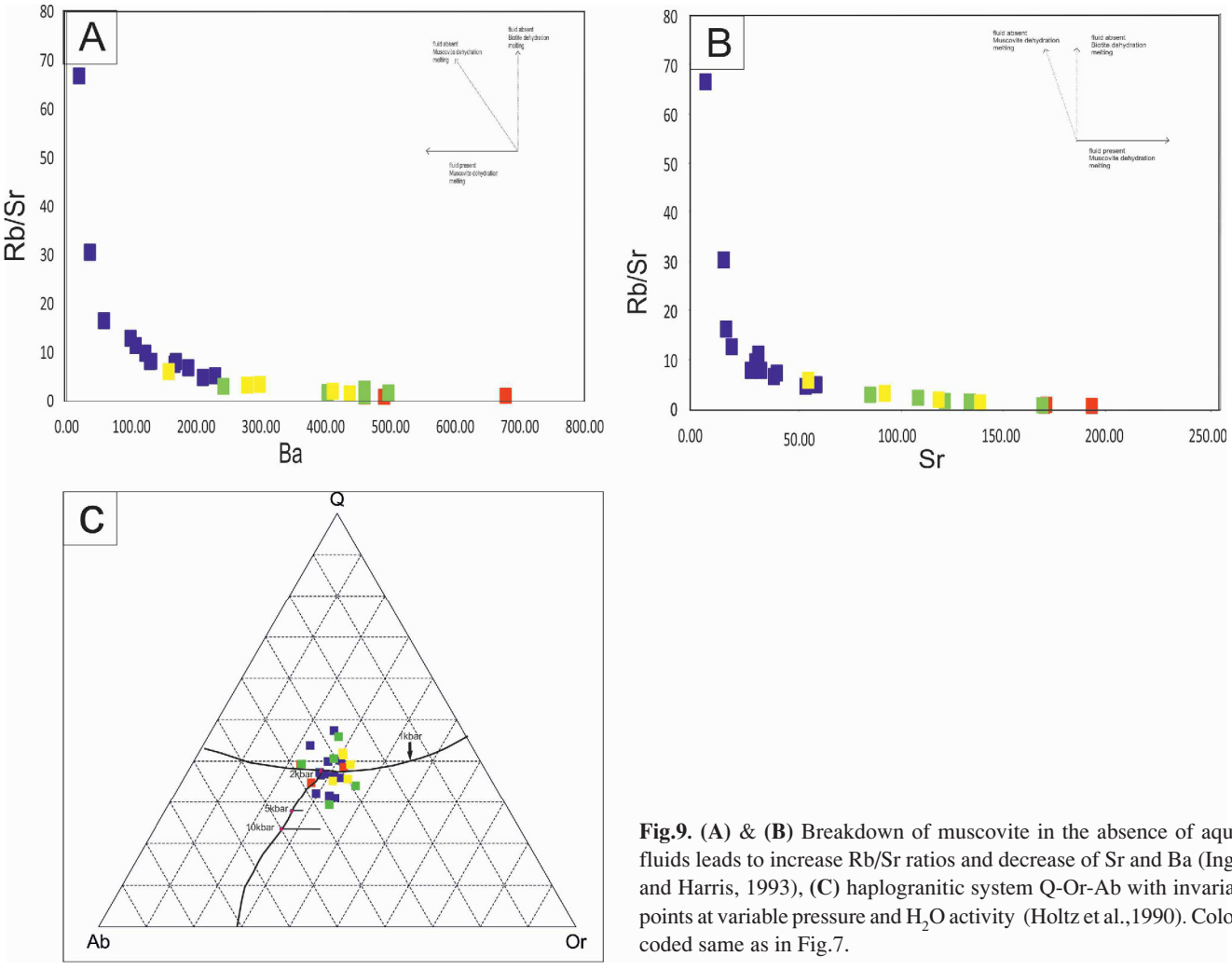

Fig.9. (A) & **(B)** Breakdown of muscovite in the absence of aquas fluids leads to increase Rb/Sr ratios and decrease of Sr and Ba (Inger and Harris, 1993), **(C)** haplogranitic system Q-Or-Ab with invariant points at variable pressure and H_2O activity (Holtz et al.,1990). Colour coded same as in Fig.7.

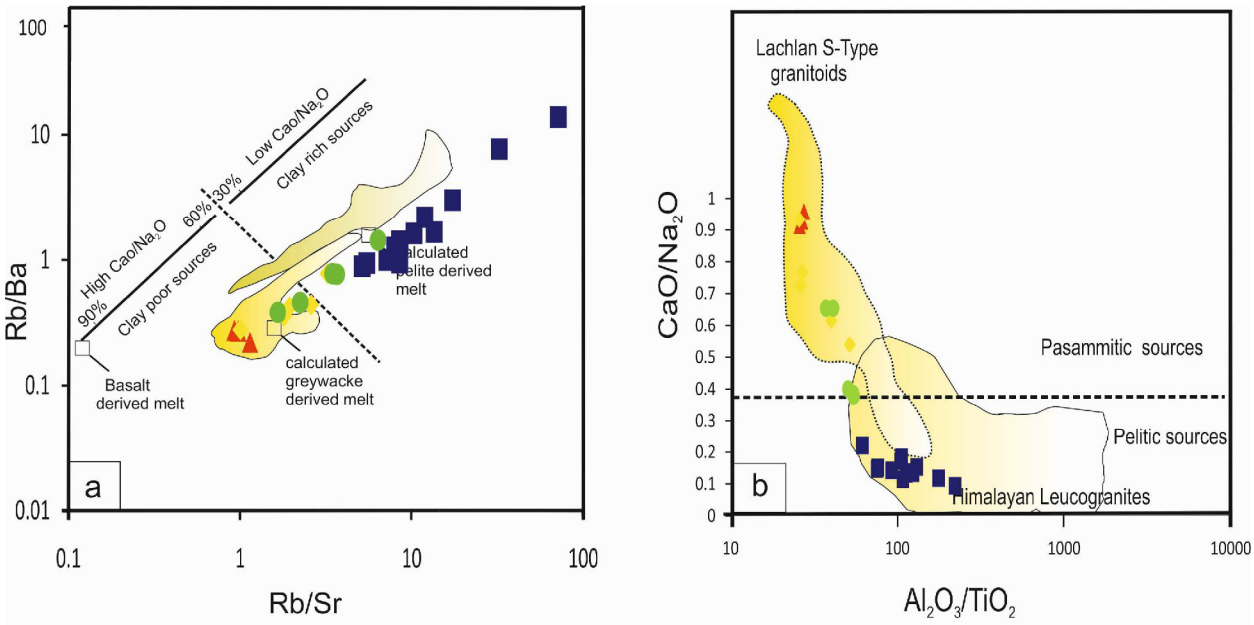

Fig.10. Interpretation of source rock composition **(A)** Rb/Ba versus Rb/Sr diagram, calculated source composition after Sylvester (1998) **(B)** Al_2O_3/TiO_2 versus Cao/Na_2O, indicates the field of strongly peraluminous Sylvester (1998). Colour coded same as Fig.7.

fractionation behavior also provides an indication of melting conditions. Dalhousie granites exhibit higher Rb/Sr ratios (4.9-66.9), low Sr and Ba, a pronounced Eu anomaly and fall along the trend of muscovite dehydration melting (Inger and Harris, 1993). The Dhauladhar granites, on the other hand, show lower Rb/Sr ratios (0.9-3.3), high Sr, Ba with negligible to no Eu anomaly, suggesting water present melting (Fig. 9a,b). The higher FeO/MgO ration in the Dhauladhar suite of rocks compared to the Dalhousie rocks is also attributed to the melting in Dhauladhar area under water flux condition. The continues trend in major and trace elements vs SiO_2 (Fig.4) along with the similar primitive mantle-normalized spider diagrams and similar Chondrite-normalized REE patterns indicate that these granites were formed from a common source by the plagioclase fractionation under fluid-absent and present conditions. The Q-Ab-Or diagram suggests that these granites belong to the eutectics of the haplogranite system having H_2O in the system with 2 and 5 Kbar pressure (Holtz et al,1992; Holtz et al,1994).

The high Rb (<500) and low Sr and Ba in the Dalhousie granites indicate that the crystal fractionation was likely the main process of the magma evolution. In contrast, Dhauladhar has lower Rb (< 352) higher Sr and Ba contents. These observations imply that plagioclase fractionation is more prominent in Dalhousie granites than Dhauladhar granites. Plagioclase fractionation has resulted in depletion of Eu from the evolved melt which has been manifested in the form of a pronounced negative Eu anomaly. Dhauladhar granites show less pronounced to no Eu anomaly. Some studies (Bea et al., 2006; Zaraysky et al., 2007) have used the Zr/Hf ratio as granite fractionation index. Zr/Hf decreases with increasing evolution of a silicate melt (e.g. Irber, 1999). High Zr/Hf ratios in Dhauladhar granite (2.1-9) compared to Dalhousie granite (0.3-0.8) indicates that the Dalhousie granites are more evolved than Dhauladhar granites. The fractionation process can also be identified by the use of log-log plots (Fig. 11) (Allègre and Minster, 1978). The log-plots (Fig. 11) involving Rb, Sr, Eu/Eu* and Ba illustrate the importance of K-feldspar and plagioclase fractionation, and also for biotite fractionation. These plots show that Dhauladhar samples show a shorter range of fractionation or less fractionation controlled by biotite. In Dalhousie, samples extended fractionation controlled by K-feldspar and plagioclase has produced the variation in Sr, Ba, and Eu and a negative Eu anomaly

CONCLUSIONS

Present work indicates that both the Dalhousie and Dhauladhar

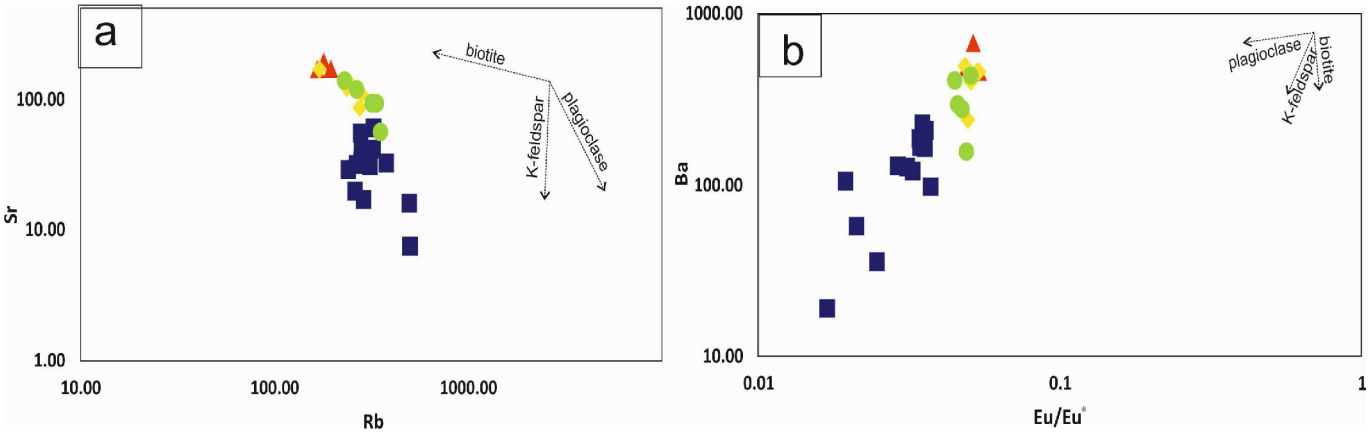

Fig.11. (A) Rb vs. Sr, **(B)** Eu/Eu* vs. ba – log-log diagrams that indicate the role of rock-forming minerals in the fractional crystallization. In (A) vectors of fractional crystallization for K-feldspar, plagioclase, and biotite (breaks and Moore (1992), and (B) (Landerberger and Collins 1996). Colour coded same as Fig.7.

granites are strongly peraluminous, silica-rich S-type granites, formed from partial melting and crystallization of a metasedimentary source. The detailed geochemical characteristics of these granites do not define a single unit, rather indicate the complex history in which two contrasting granites were formed. Partial melting of a meta-psammitic source by muscovite dehydration melting in presence of water has generated the granitic melt for Dhauladhar granites. Melt evolution by fractionation has involved mostly biotite; feldspar has played a minor role. In contrast, the melt for the Dalhousie granites has been generated from a meta-pelitic source by muscovite dehydration melting in the absence of water. Dalhousie granites are more evolved and fractionated than Dhauladhar granites. Plagioclase fractional crystallization has played a major role in the evolution of Dalhousie granitic melt.

Acknowledgments : We are thankful to Heads, Department of Earth Sciences, and Institute Instrumentation Center, IITR Roorkee and the Director, Wadia Institute of Himalayan Geology, for extending the facilities to take up this work. RD is also thankful to the University Grants Commission for the grant (Grant no. 6405-14-044-428) and SS thanks Ministry of Earth Sciences for a research project (grant no. MoEs-P.O.(Geosci)/27/2014). Comments of an anonymous reviewer helped in improving the initial manuscript.

References

Allegre, C.J. and Minster, J.F. (1978) Quantitative models of trace element behavior in magmatic processes. Earth Planet. Sci. Lett., v.38(1), pp.1-25.

Bea, F., Montero, P. G., Gonzalez-Lodeiro, F., Talavera, C., Molina, J. F., Scarrow, J. H., ... and Zinger, T. (2006) Zircon thermometry and U–Pb ion-microprobe dating of the gabbros and associated migmatites of the Variscan Toledo Anatectic Complex, Central Iberia. Jour. Geol. Soc. London, v.163(5), 847-855

Bhatia, G.S. and Kanwar, R.C. (1973) Mylonitization in outer Granite Band of Dalhousie, Himachal Pradesh. Himalayan Geol., v.3 pp.103-115

Bhatia, G.S. (1975) Contribution to the Geology of Dalhousie Chamba area Himachal Pradesh, India.

Cawood, P.A., Johnson, M.R. and Nemchin, A.A. (2007) Early Palaeozoic orogenesis along the Indian margin of Gondwana: Tectonic response to Gondwana assembly. Earth Planet. Sci. Lett., v.255(1-2), pp.70-84. doi: 10.1016/j.epsl.2006.12.006.

Chappell, B.W. and White, A.J.R. (1992) I-and S-type granites in the Lachlan Fold Belt. Earth and Environmental Science Transactions of the Royal Society of Edinburgh, v.83(1-2), pp.1-26. doi:10.1017/S0263593300007720

Chappell, B.W. and White, A.J. (2001) Two contrasting granite types: 25 years later. Australian Jour. Earth Sci., v.48(4), pp.489-499. doi:10.1046/j.1440-0952.2001.00882.x

Chaudhri, N. (1996) Geochemistry and petrogenesis of the Palampur Granitoids, Dhauladhar range, northwestern Himalaya, India. Chemie Der Erde -Geochemistry, v.56(1), pp.25-43.

Clemens, J.D. (2003) S-type granitic magmas—petrogenetic issues, models and evidence. Earth-Science Rev., pp.61(1-2), pp.1-18.

Clemens, J.D. and Stevens, G. (2012) What controls chemical variation in granitic magmas?. Lithos, v.134, pp.317-329. doi:10.1016/j.lithos.2012.01.001

Collins, W. J. and Sawyer, E.W. (1996) Pervasive granitoid magma transfer through the lower–middle crust during non coaxial compressional deformation. Jour.Metamor. Geol., v.14(5), doi:10.1046/j.1525-1314.1996.00442.x

Conrad, W.K., Nicholls, I.A. and Wall, V.J. (1988) Water-saturated and-undersaturated melting of metaluminous and peraluminous crustal compositions at 10 kb: evidence for the origin of silicic magmas in the Taupo Volcanic Zone, New Zealand, and other occurrences. Jour. Petrol., v.29(4), pp.765-803.

DeCelles, P. G., Gehrels, G. E., Quade, J., LaReau, B. and Spurlin, M. (2000) Tectonic implications of U-Pb zircon ages of the Himalayan orogenic belt in Nepal. Science, v.288(5465), pp.497-499.

DePaolo, D. J. (1981). Trace element and isotopic effects of combined wallrock assimilation and fractional crystallization. Earth Planetary Sci. Lett., v.53(2), 189-202.

Frank,W., Thoni, M. and Purtscheller, F. (1977) Geology and petrography of Kullu-South Lahul area. – Colloques Internationaux du C.N.R.S., v. 286, pp.147–172.

Frost, B.R. and Frost, C.D. (2013) Essentials of igneous and metamorphic petrology. Cambridge University Press

Gao, L.E. and Zeng, L. (2014) Fluxed melting of metapelite and the formation of Miocene high-CaO two-mica granites in the Malashan gneiss dome, southern Tibet. Geochim. Cosmochim. Acta, v.130, pp.136-155.

Harris, N.B.W. and Inger, S. (1992) Trace element modelling of pelite-derived granites. Contrib. Mineral. Petrol., v.110(1), 46-56. doi:10.1007/BF00310

Healy, B., Collins, W.J. and Richards, S.W. (2004) A hybrid origin for Lachlan S-type granites: the Murrumbidgee Batholith example. Lithos, v.78(1-2), pp.197-216. doi:10.1016/j.lithos.2004.04.047

Holtz, F., Behrens, H., Dingwell, D.B. and Taylor, R.P. (1992) Water solubility in aluminosilicate melts of haplogranite composition at 2 kbar. Chemical Geol., v.96(3-4), pp.289-302.

Holtz, F. and Johannes, W. (1994) Maximum and minimum water contents of granitic melts: implications for chemical and physical properties of ascending magmas. Lithos, v.32(1-2), 149-159. doi:10.1016/0024-4937(94)90027-2

Inger, S. and Harris, N. (1993) Geochemical constraints on leucogranite magmatism in the Langtang Valley, Nepal Himalaya. Jour. Petrol., 34(2), pp.345-368. doi:10.1093/petrology/34.2.345.

Irber, W. (1999) The lanthanide tetrad effect and its correlation with K/Rb, Eu/Eu", Sr/Eu, Y/Ho, and Zr/Hf of evolving peraluminous granite suites. Geochim. Cosmochim. Acta, v.63(3-4), pp.489-508.

Irvine, T. N. J. and Baragar, W.R.A. (1971) A guide to the chemical classification of the common volcanic rocks. Canadian Jour. Earth Sci., v.8(5), pp.523-548.

Jung, S. and Pfander, J. A. (2007) Source composition and melting temperatures of orogenic granitoids: constraints from CaO/Na_2O, Al_2O_3/TiO_2 and accessory mineral saturation thermometry. European Jour. Mineral., v.19(6), pp.859-870. doi:10.1127/0935-1221/2007/0019-1774

Kemp, A.J. and Hawkesworth, C.J. (2003) Granitic Perspectives on the Generation and Secular Evolution of the Continental Crust. *In:* R.L. Rudnick (Ed.), The Crust (Treatise on Geochemistry, Vol 3) (pp. 349 - 410). Amsterdam: Elsevier.

Kansal, A. K., Singh, V. P., Anupam, K., & Bhanot, V. B. (2003) Rb-Sr isotopic and geochronological studies of the granitic rocks of Dalhousie area, Himachal Pradesh. *In:* ISMAS silver jubilee symposium on mass spectrometry. V.2: contributed papers.

Lahoti, S., Kumud, K., Gupta, Y. and Jain, A.K. (2017) Tectonics of the Chamba Nappe, NW Himalaya and its regional implications. Italian Jour. Geosci., v.136, pp.50-63. doi: 0.3301/IJG.2015.39

Le Fort, P. (1983) The lower Paleozoic "Lesser Himalayan" granitic belt: emphasis on the Simchar pluton of Central Nepal. Granites of Himalayas, Karakorum and Hindu Kush, pp.235-255.

Le Fort, P. (1986) The 500 Ma magmatic event in Alpine southern Asia, a thermal episode at Gondwana scale. Evolution des Domaines *Orogeniques d'Asie Meridionale*, 47, 191-209.

Le Fort, P., Cuney, M., Deniel, C., France-Lanord, C., Sheppard, S.M.F., Upreti, B. N. and Vidal, P. (1987) Crustal generation of the Himalayan leucogranites. Tectonophysics, v.134(1-3), pp.39-57. doi:10.1016/0040-1951(87)90248-4

McMahon, C.A. (1881) Note on the section from Dalhousie to Pangi via Sach Pass. Rec. Geol. Surv. India, v.14, pp.305-310.

Miller, C., Thöni, M., Frank, W., Grasemann, B., Klötzli, U., Guntli, P. and Draganits, E. (2001) The early Palaeozoic magmatic event in the Northwest Himalaya, India: source, tectonic setting and age of emplacement. Geol. Magz., v.138(3), pp.237-251.

Mukherjee, P.K., Purohit, K.K., Rathi, M.S. and Khanna, P.P., (1998) Geochemistry and Petrogenesis of a Supracrustal Granite from Dalhousie, Himachal Himalaya. Jour. Geol. Soc. India, v.52, pp.163-180.

Nautiyal, S.P., Dhoundhial, D.P., Nadgir,B.B., Das Gupts, S.P. and Ramachanndra, A.V. (1952) Suitability of the Dharakot Limestone for Portland cement manufacture, Kangra, H.P. Rec. Geol. Surv. India, v.87(4), pp.707–750.

Patino Douce, A. E. (1997) Generation of metaluminous A-type granites by

low-pressure melting of calc-alkaline granitoids. Geology, v.25(8), pp.743-746. doi:10.1130/0091-7613.

Patino Douce, A. E. (1999). What do experiments tell us about the relative contributions of crust and mantle to the origin of granitic magmas? Geol. Soc. London, Spec. Publ., v.168(1), pp.55-75. doi:10.1144/GSL.SP.1999.168.01.05

Patino Douce, A.E. and Beard, J.S. (1996). Effects of P, f(O_2) and Mg/Fe ratio on dehydration melting of model metagreywackes. Jour. Petrol., v.37(5), pp.999-1024.

Rollinson, H.R. (2014) Using geochemical data: evaluation, presentation, interpretation. Routledge

Satyanarayanan, M., Balaram, V., Sawant, S.S., Subramanyam, K.S.V. and Krishna, G.V. (2014) High precision multielement analysis on geological samples by HR-ICPMS. In 28th ISMAS Symposium Cum Workshop on Mass Spectrometry. Indian So. Mass Spectrometry, Mumbai, India, pp.181-184

Singh, S. and Jain, A.K. (1996). Ductile shearing of the Proterozoic Chor Granitoid in the Lesser Himalaya and its tectonic significance. Jour. Geol. Soc. India, v.47(1), pp.133-138.

Singh, S. and Jain, A.K. (2003). Himalayan granitoids. Jour. Virtual Explorer, v.11, pp.1-20.

Singh, J. and Johannes, W. (1996) Dehydration melting of tonalites. Part I. Beginning of melting. Contrib. Mineral. Petrol., v.125(1), pp.16-25.

Singh, S. (2003) Conventional and SHRIMP U-Pb Zircon Dating of the Chor Granitoid, Himachal Himalaya. Jour. Geol. Soc. India, v.62, pp.614-626.

Singh, S. (2005) A review of U–Pb ages from Himalayan Collisonal Belt. Jour. Himalayan Geol., v.26, pp.61-76.

Singh, S., Barley, M.E., Brown, S.J., Jain, A.K. and Manickavasagam, R.M. (2002) SHRIMP U–Pb in zircon geochronology of the Chor granitoid: evidencefor Neoproterozoic magmatism in the Lesser Himalayan granite belt of NW India. Precambrian Res., v.118, pp.285-292. doi:10.1016/S0301-9268(02)00107-9

Sun, S.S. and McDonough, W.S. (1989) Chemical and isotopic systematics of oceanic basalts: implications for mantle composition and processes. Geol. Soc., London, Spec. Publ., v.42(1), pp.313-345.

Sylvester, P.J. (1998) Post-collisional strongly peraluminous granites. Lithos, v.45(1-4), pp.29-44. doi:10.1016/S0024-4937(98)00024-3

Thakur, V.C., Rautela, P. and Jafaruddin, M. (1995). Normal faults in Panjal thrust zone in lesser Himalaya and between the higher Himalaya crystallines and Chamba sequence in Kashmir Himalaya, India. Proc. Indian Acad. Sci. EarthPlanet. Sci., v.104(3), pp.499-508.

Thirlwall, M.F. and Jones, N.W. (1983) Isotope geochemistry and contamination mechanics of Tertiary lavas from Skye, Northwest Scotland. Continental basalts and mantle xenoliths, pp.186-208.

Watkins, J.M., Clemens, J.D. and Treloar, P.J. (2007) Archaean TTGs as sources of younger granitic magmas: melting of sodic metatonalites at 0.6–1.2 GPa. Contrib. Mineral. Petrol., v.154(1), pp.91-110.

Weinberg, R.F. and Hasalová, P. (2015) Water-fluxed melting of the continental crust: A review. Lithos, v.212, pp.158-188.

Zaraysky, G.P., Alfereva, J.O. and Udoratina, O.V. (2007) Geochemical features of the tantalum deposit in Eastern Transbaikalia Etyka. *In:* Sixth International Hutton Symposium. Origin of granites and related rocks. Abstract. Stellenbosch, South Africa (pp. 232-233).

Zheng, Y.F., Zhou, J.B., Wu, Y.B. and Xie, Z. (2005) Low-grade metamorphic rocks in the Dabie-Sulu orogenic belt: A passive-margin accretionary wedge deformed during continent subduction. Internat. Geol. Rev., v.47(8), pp.851-871. doi:10.2747/0020-6814.47.8.851.

(Received: 26 March 2018; Revised form accepted: 27 August 2018)